Role of a New Mammalian Gene Family in the Biosynthesis of Very Long Chain Fatty Acids and Sphingolipids

Petr Tvrdik,* Rolf Westerberg,* Sandra Silve,‡ Abolfazl Asadi,* Andreas Jakobsson,* Barbara Cannon,* Gerard Loison,‡ and Anders Jacobsson*

*The Wenner-Gren Institute, The Arrhenius Laboratories F3, Stockholm University, SE-106 91 Stockholm, Sweden;
‡Department of Microbiology, Sanofi Recherche, Labège Innopole BP137, F-31676 Labège Cédex, France

Abstract. Whereas the physiological significance of microsomal fatty acid elongation is generally appreciated, its molecular nature is poorly understood. Here, we describe tissue-specific regulation of a novel mouse gene family encoding components implicated in the synthesis of very long chain fatty acids. The *Ssc1* gene appears to be ubiquitously expressed, whereas *Ssc2* and *Cig30* show a restricted expression pattern. Their translation products are all integral membrane proteins with five putative transmembrane domains. By complementing the homologous yeast mutants, we found that *Ssc1* could rescue normal sphingolipid synthesis in the *sur4*/*elo3* mutant lacking the ability to synthesize cerotic acid ($C_{26:0}$). Similarly, *Cig30* reverted the phenotype of the *fen1*/*elo2* mutant that has reduced levels of fatty acids in the C_{20}–C_{24} range. Further, we show that *Ssc1* mRNA levels were markedly decreased in the brains of myelin-deficient mouse mutants known to have very low fatty acid chain elongation activity. Conversely, the dramatic induction of *Cig30* expression during brown fat recruitment coincided with elevated elongation activity. Our results strongly implicate this new mammalian gene family in tissue-specific synthesis of very long chain fatty acids and sphingolipids.

Key words: membrane • lipids • elongation • myelin • gene expression

Introduction

Fatty acid species with a maximum chain length of 16–18 carbon atoms account for >90% of total fatty acids in most mammalian tissues. However, many biological processes depend on fatty acids consisting of 20 and more carbon atoms, which are generally referred to as very long chain fatty acids (VLCFA)[1]. Although virtually ubiquitous, VLCFA are found at especially high levels in the brain, skin, testis, and some glands, such as the meibomian gland (for review see Poulos, 1995).

Only a very small fraction of VLCFA occurs unesterified; the main fraction of intracellular VLCFA is esterified in various lipids. Under normal circumstances, a substantial amount of VLCFA is amide-linked to a long-chain sphingoid base sphinganine, forming a ceramide, which constitutes the lipid backbone of sphingomyelin and other sphingolipids. Apparently, the distribution bias for VLCFA between sphingolipids and e.g., glycerolipids is controlled by substrate specificity of the corresponding fatty acyltransferases, such as ceramide synthase.

Sphingolipids are essential for cell proliferation. Impaired sphingolipid synthesis leads to cessation of cell growth both in yeast (Wells and Lester, 1983) and mammalian cells (Hanada et al., 1992). Unique structural properties of sphingolipids strongly contribute to the epidermal water barrier (Wertz, 1992), as well as enhance electric insulation of myelin (Bourre et al., 1977). The bulk of sphingolipids are located in the plasma membrane, permitting the complex sugar groups of glycosphingolipids to act in cell recognition and adhesion (Hakomori and Igarashi, 1995). A large body of evidence has been accumulated that implicates sphingolipids and their degradation products in signal transduction (Hannun, 1996; Spiegel and Merrill, 1996; Testi, 1996) and formation of functional lipid microdomains in the plasma membrane (Simons and

Address correspondence to Anders Jacobsson, The Wenner-Gren Institute, The Arrhenius Laboratories F3, Stockholm University, SE-106 91 Stockholm, Sweden. Tel.: +46-8-164127. Fax: +46-8-156756. E-mail: anders.jacobsson@wgi.su.se

Petr Tvrdik's present address is Howard Hughes Medical Institute, University of Utah, 15 North 2030 East, Salt Lake City, UT 84112-5331. Tel.: (801) 581-7097. Fax: (801) 585-3425. E-mail: petr.tvrdik@genetics.utah.edu

Sequence data have been deposited with GenBank/EMBL/DDBJ under accession nos. AF170907 and AF170908.

[1]*Abbreviations used in this paper:* IPC, inositolphosphorylceramide; MIPC, mannose IPC; $M(IP)_2C$, mannose diinositolphosphorylceramide; *Ssc*, sequence similarity to *Cig30*; VLCFA, very long chain fatty acids.

Ikonen, 1997). Interestingly, suppressor mutations in sphingolipid-deficient yeast mutants have demonstrated that glycerophospholipids containing VLCFA can mimic sphingolipid structures, allowing yeast growth in the absence of sphingolipid (Lester et al., 1993). Hence, VLCFA appears to be an essential component of sphingolipid function.

It is well established that the major site of VLCFA synthesis beyond C_{18} occurs on the membranes of the ER (Cinti et al., 1992). The elongation process is similar to the series of reactions carried out by fatty acid synthase and involves four steps: condensation, reduction, dehydration, and a second reduction. It is unclear whether all elongation reactions are accomplished by a single polypeptide, or rather by a complex of several subunits. However, several discrete enzymatic activities, e.g., β-hydroxyacyl CoA dehydrase, have been purified to high homogeneity (Bernert and Sprecher, 1979), suggesting that the latter possibility is more likely. Another long-standing question has been whether or not multiple microsomal elongation systems exist in the cell with different saturation and/or chain length specificities. This notion emerged from studies performed on myelin-deficient mouse mutants, namely jimpy and quaking. In the brains of these mice, arachidoyl CoA (C_{20}) and behenoyl CoA (C_{22}) elongation activities are decreased more dramatically than palmitoyl CoA (C_{16}) elongation (Suneja et al., 1991), supporting the concept of multiple elongation pathways.

To date, very little is known about the genetic nature of mammalian fatty acid chain elongation enzymes. Several putative condensing enzymes involved in VLCFA biosynthesis have been cloned and characterized in plants (Millar and Kunst, 1997; Millar et al., 1999). In yeast, which are more akin to mammals in terms of the biochemical roles of VLCFA, the *ELO* gene family appears to be indispensable for fatty acid chain elongation. The first homologue of this group, *ELO1*, is required for microsomal fatty acid chain elongation between C_{14} and C_{16} (Toke and Martin, 1996), an activity which is normally masked by cytoplasmic fatty acid synthase. The other two *ELO* genes, *ELO2* and *ELO3*, are necessary for synthesis of VLCFA of up to 24 and 26 carbon atoms, respectively (Oh et al., 1997). For the reasons mentioned above, low VLCFA levels result in a dramatic decrease of all three principal sphingolipid species normally found in *Saccharomyces cerevisiae*, i.e., inositolphosphorylceramide [IPC], mannose inositolphosphorylceramide [MIPC] and mannose diinositolphosphorylceramide [$M(IP)_2C$] (Oh et al., 1997). Consequently, low sphingolipid levels might be the primary cause of the pleiotropic phenotypes associated with mutations in these loci. In fact, disruption of either of *ELO2* or *ELO3*, that have been cloned by different groups and synonymically termed *FEN1/GNS1/SRE2/VBM2* and *SUR4/APA1/SRE1/VBM1*, leads to a broad range of defects, encompassing altered expression of the plasma membrane ATPase gene and lowered glucose uptake capacity (García-Arranz et al., 1994), marked reduction in 1,3-β-glucan synthase activity (El-Sherbeini and Clemas, 1995), modified phospholipid composition (Desfarges et al., 1993), irregular budding pattern (Durrens et al., 1995), and resistance to inhibitors of sterol synthesis (Ladeveze et al., 1993; Silve et al., 1996). Moreover, mutation in either of these genes also suppresses the phenotype of the *rvs* mutant, which is characterized by reduced viability upon nitrogen, carbon, or sulfur starvation (Desfarges et al., 1993), and bypasses a defect in the receptor-mediated secretory pathway, restoring normal exocytosis (David et al., 1998). Simultaneous disruption of *ELO2/FEN1/GNS1/SRE2/VBM2* and *ELO3/SUR4/APA1/SRE1/VBM1* (which, in accordance with the *S. cerevisiae* Gene Name Registry, will henceforth be referred to as *FEN1* and *SUR4*) is lethal (Revardel et al., 1995; Silve et al., 1996). If the central tenet about primary function of these genes holds, the data accumulated in these studies could provide new and profound insight into the complexity of the role(s) of VLCFA and sphingolipids in the cell.

Previously, we have reported our finding of *Cig30*, a highly inducible mouse gene, the expression of which is associated with the activity of brown adipose tissue (Tvrdik et al., 1997). The CIG30 protein is very similar to *FEN1* and *SUR4* gene products, but also to a number of genes identitified in the genome of *Caenorhabditis elegans*. Assuming the presence of multiple genes of this family in the mouse genome as well, we searched for *Cig30* homologues and identified two novel genes, which were designated *Ssc1* and *Ssc2* (for sequence similarity to *Cig30*). We present evidence that the members of this mouse gene family participate in the process of VLCFA synthesis.

Materials and Methods

Animals and Treatments

For comparison of *Ssc1*, *Ssc2*, and *Cig30* expression profiles and for fatty acid chain elongation studies, NMRI male mice (6–8 wk old) were obtained from a local supplier (Eklunds) and kept at thermoneutral temperature (28°C) for 1 wk. After this period, some animals were exposed to 4°C when indicated. The mice were killed by cervical dislocation and the tissues were dissected and directly subjected to RNA extraction or homogenization and differential centrifugation.

To analyze cerebral *Ssc1* mRNA levels in dysmyelinating mutants, heterozygous breeder pairs of quaking (B6C3Fe-*a/a-qk*) and jimpy (B6CBACa-$A^{w\text{-}J}$/A-*Ta jp*) were obtained from the Jackson Laboratory and bred in our animal facility. The mutant pups and their healthy littermate controls were killed at the age of 18 d and their brains were quickly dissected and frozen in liquid nitrogen before RNA extraction.

Mouse cDNA Cloning and Sequencing

Based on sequence information obtained from the EST sequencing project, primers were designed to PCR amplify the protein coding regions of *Ssc1*, *Ssc2*, and *Cig30* from mouse liver Marathon-Ready cDNA library (Clontech). The primers used were: primer 1, 5′-GGACGTCGACTGAGTCCTTAGCCAGGATGGAGGCTGTTGT-3′ and primer 2, 5′-GAGCAGATCTGTCCTGAGGCACTTAGGTGGGCAATGTCTA-3′ for *Ssc1* ORF amplification; primer 3, 5′-GGACGTCGACCGCGGCCGCGCGGCCATGGAGCAGCTGAA-3′ and primer 4, 5′-GAGCAGATCTCCACCTCAGTTTGTGTTCCCCGGCACTTCA-3′ for *Ssc2* ORF amplification; and primer 5, 5′-GGACGTCGACCGTCTGCAAAATCGAAATGGACACATCCAT-3′ and primer 6, 5′-GAGCAGATCTACGGAGGAACGGCTGAGGCTCCATCTTTCT-3′ for *Cig30* ORF amplification. To facilitate cloning, all forward primers contain exogenous SalI sites and all reverse primers contain exogenous BglII sites (both shown in bold face). The touch-down PCR reactions were performed with the *Pfu* polymerase (Stratagene) for 32 cycles totally (after denaturation at 94°C for 1 min, 5 cycles 94°C for 30 s, 72°C for 3 min, 5 cycles 94°C for 30 s, 70°C for 3 min, and 22 cycles 94°C for 30 s, 68°C for 3 min). For each gene, at least two independent PCR products were sequenced to check that no amplification errors occurred. To obtain the full-length mRNA sequences of *Ssc1* and *Ssc2*, RACE experiments were performed using primer 7, 5′-GGCTATTGGAAAAGTCTATGGGGT-

CACA-3′ for *Ssc1* 5′ RACE; primer 8, 5′-GGCACCATCTTCTTCAT-ACTGTTCTCCA-3′ for *Ssc1* 3′ RACE; primer 9, 5′-CCAGCATA-TACGCAGAAAGAAGTGTG-3′ for *Ssc2* 5′ RACE; and primer 10, 5′-GACATACCGGAAAAAGCCAGTGAAGAAA-3′ for *Ssc2* 3′ RACE. The template and PCR conditions were the same as above. 5′ RACE experiments were run for each *Ssc* transcript twice with identical results. The PCR products were subcloned into pCR-XL-TOPO vector (Invitrogen) and sequenced using ABI Prisms Dye Terminator Cycle Sequencing Ready Reaction kit (Perkin-Elmer) with an ABI 373A automatic DNA sequencer (Applied Biosystems). Sequence data analyses were performed with the University of Wisconsin Genetics Computer Group package (Devereux et al., 1984).

RNA Isolation and Northern Blotting

Total RNA was isolated from fresh or frozen specimens of mouse tissues (~50 mg) using the Ultraspec RNA isolation protocol (Biotecx Laboratories). RNA electrophoresis, blotting, and hybridization was performed as previously described (Tvrdik et al., 1997). The cDNA probes for *Ssc1*, *Ssc2*, and *Cig30* were SalI–BglII fragments isolated from their corresponding pEMR yeast expression vectors. The actin probe was as in Tvrdik et al. (1997). The probes were labeled using random-primed DNA labeling kit (Boehringer Mannheim) with [^{32}P]dCTP.

Yeast Strains and Culture Conditions

Yeast strains used in this study and their genotypes are presented in Table I. They are all FL100 (ATCC 28383) derivatives. For metabolic labeling and growth studies, all strains were grown on YNBG medium (Difco), supplemented with tryptophane (EMA41 transformants), tryptophane and leucine (EMY58 transformants), and tryptophane and uracil (EMA3). For EMA103 strain, YNBG medium was supplemented with 1% Tergitol, myristic acid (C_{14}, 0.2 mM), palmitic acid (C_{16}, 0.4 mM), and stearic acid (C_{18}, 0.2 mM). EMA103 transformants were grown on medium supplemented with Tergitol and C_{14} only. Alternatively, EMY58 transformants were grown on YPGE medium, containing 2% bactopeptone (Difco), 1% yeast extract (Difco), 3% glycerol, and 1% ethanol.

Yeast Plasmids and DNA Manipulation

pEMR1023, a multicopy plasmid containing the selection marker *URA3*, was described previously (Silve et al., 1996). The coding sequences of *Ssc1*, *Ssc2*, and *Cig30* were obtained by PCR amplification as described above, digested with SalI and BglII, and ligated in the SalI and BglII sites of the pEMR1023 vector. The pNK451 plasmid was used to disrupt the *FAS2* gene according to Alani et al. (1987). Yeast transformation was carried out as described (Gietz et al., 1992).

The *SUR4* gene deletion was made as follows: the 1.1-kb PvuII–HpaI fragment in the coding region of *SUR4* was replaced by a 1.4-kb DraI–MluI fragment, which contained the *neo* gene derived from transposon Tn903. The resulting plasmid was digested with BamHI, and the 3.2-kb fragment encompassing the disruption was used to transform EMY30 cells. Successful *SUR4* gene replacement in geneticin-resistant cells was checked by PCR analysis. Disruptant cells (EMY58) were resistant to 200 μg/ml geneticin and 25 μM SR 31747.

To disrupt the *FAS2* gene in the *elo1* mutant (EMA45), a knockout vector was constructed in which two *FAS2* genomic regions (corresponding to the promoter and terminator, respectively, nucleotides 830–1,350 and 2,130–2,160, GenBank/EMBL/DDBJ accession no. J03936) were PCR-cloned and inserted in the EcoRI/BglII and BamHI/SalI sites of the pNK451 vector to flank the HisG-*URA3*-HisG sequence. Next, the MluI–EcoRI fragment encompassing the *FAS2*-HisG-*URA3*-HisG-*FAS2* cassette was gel-purified and transfected into EMA45. Three colonies were obtained that were able to grow on synthetic medium supplemented with Tergitol (1% wt/vol), C_{14} (0.2 mM), C_{16} (0.4 mM), and C_{18} (0.2 mM), but not on medium supplemented with Tergitol and C_{14} only. The *URA3* marker was then eliminated via HisG–HisG recombination by incubation in the presence of 5′-fluoroorotic acid (1 mg/ml) and uracil, yielding EMA103. Deletion of the *FAS2* gene in EMA103 was finally verified by PCR and Southern blot analyses.

Table I. Yeast Strains Used in this Study

Strain	Genotype	Source or reference
EMA3	*Mat***a** *ura3 trp1*	François Lacroute*
EMA41	*Mat***a** *ura3 trp1 leu2 fen1::LEU2*	Silve et al., 1996
EMA45	*Mat***a** *ura3 trp1 elo1::TRP1*	Pascal Leplatois*
EMA103	*Mat***a** *ura3 trp1 elo1::TRP1* Δ*FAS2*	This study
EMY22	*Matα ura3 sur4*-232	Silve et al., 1996
EMY30	*Matα ura3 trp1 leu2*	Silve et al., 1996
EMY58	*Matα ura3 trp1 leu2 sur4::GenR*	This study

*Sanofi Recherche, Labège Innopole, France.

Sphingolipid Analysis

Overnight cultures of yeast transformants were diluted to ~2×10^6 cells/ml (OD_{600} = 0.066) and grown in 2 ml of appropriately supplemented YNBG at 30°C in the presence of the radioactive precursor. [^{3}H]serine (Nycomed Amersham; 20 μCi/ml) was added immediately after dilution and the cells were labeled for 6 h. [^{3}H]sphinganine and [^{3}H]inositol (American Radiolabeled Chemicals Inc.; each at 1 μCi/ml in the total chemical concentration of 10 μM) were added 4.5 h after dilution and the cells were labeled for 1.5 h. Incubations were terminated by chilling on ice and 0.5 ml of unlabeled stationary phase cells was added. The cultures were sedimented at 2,800 *g* for 10 min at 4°C, treated with 5% TCA at 4°C for 20 min, and were then washed once with 5 ml of ice-cold H_2O. Lipids were prepared as described (Hanson and Lester, 1980). In brief, each pellet was extracted twice with 1 ml of ethanol/water/diethyl ether/pyridine/4.2 N NH_4OH (15:15:5:1:0.018) at 60°C for 15 min. To destroy glycerophospholipids, the pooled extracts were optionally treated with 1 ml of monomethylamine reagent (33% monomethylamine in ethanol, diluted by 30% [vol/vol] with water) at 52°C for 30 min (Clarke and Dawson, 1981). The extracts were then dried in SpeedVac and dissolved in 120 μl of chloroform/methanol/water (16:16:5). 30 μl of each sample were applied to Whatman LK5D silica gel TLC plates and resolved in chloroform/methanol/4.2 NH_4OH (9:7:2). When the runs were completed, the plates were dried at 100°C for 5 min and sprayed several times with EN^{3}HANCE (New England Nuclear Life Science Products). The signal was visualized by exposing the TLC plates to DuPont Cronex X-ray films at −80°C for several weeks.

Preparation of Microsomes and Fatty Acid Elongation Assay

Interscapular brown fat was dissected and homogenized in 4 ml of ice-cold 0.25 M sucrose. After a 30-min stepwise centrifugation (10 min at each 700 *g*, 8,000 *g*, and 17,000 *g*) at 4 to 10°C, the supernatant was carefully transferred to fresh tubes and microsomes were sedimented at 105,000 *g* for 45 min. The pellet was resuspended in 20 mM Tris-HCl, pH 7.4, containing 0.4 M KCl, and centrifuged at 105,000 *g* for 45 min. The final microsomal pellet was resuspended in 200 μl of 0.1 M Tris-HCl, pH 7.4, and the protein was measured with the BCA protein assay (Pierce Chemical Co.).

Total fatty acid elongation activity was measured essentially according to Suneja et al. (1991). The assay mixtures (1 ml total, including protein addition) contained 0.1 M Tris-HCl, pH 7.4; either 50 μM palmitoyl CoA, 15 μM arachidoyl CoA, or 15 μM lignoceroyl CoA; substrate/BSA ratio of 2:1; 1 mM NADPH; and 50 μM malonyl CoA (containing 0.20 μCi of 2[^{14}C]malonyl CoA). After 1 min of preincubation at 37°C, the reaction was initiated by the addition of 1 mg of microsomal protein and carried out for 20 min at 37°C. The incubation was terminated by addition of 1 ml of 15% KOH in methanol and saponified at 65°C for 45 min. Then the samples were cooled and acidified with 1 ml of cold 5 M HCl. Free fatty acids were extracted from the mixture three times with 3 ml of *N*-hexane and dried under vacuum. The extract was dissolved in 1 ml of chloroform and measured after addition of 10 ml of scintillation mixture in a Beckman liquid scintillation system 3801.

Results

Cloning of Ssc1 and Ssc2 cDNAs

We compared the *Cig30* cDNA sequence to the EST database and found several highly similar nucleotide sequences. All mouse EST cDNA fragments seemingly conformed to two novel mRNA species. One clone of each cluster (GenBank/EMBL/DDBJ accession nos. W18104 and W48984) was acquired through the I.M.A.G.E. Con-

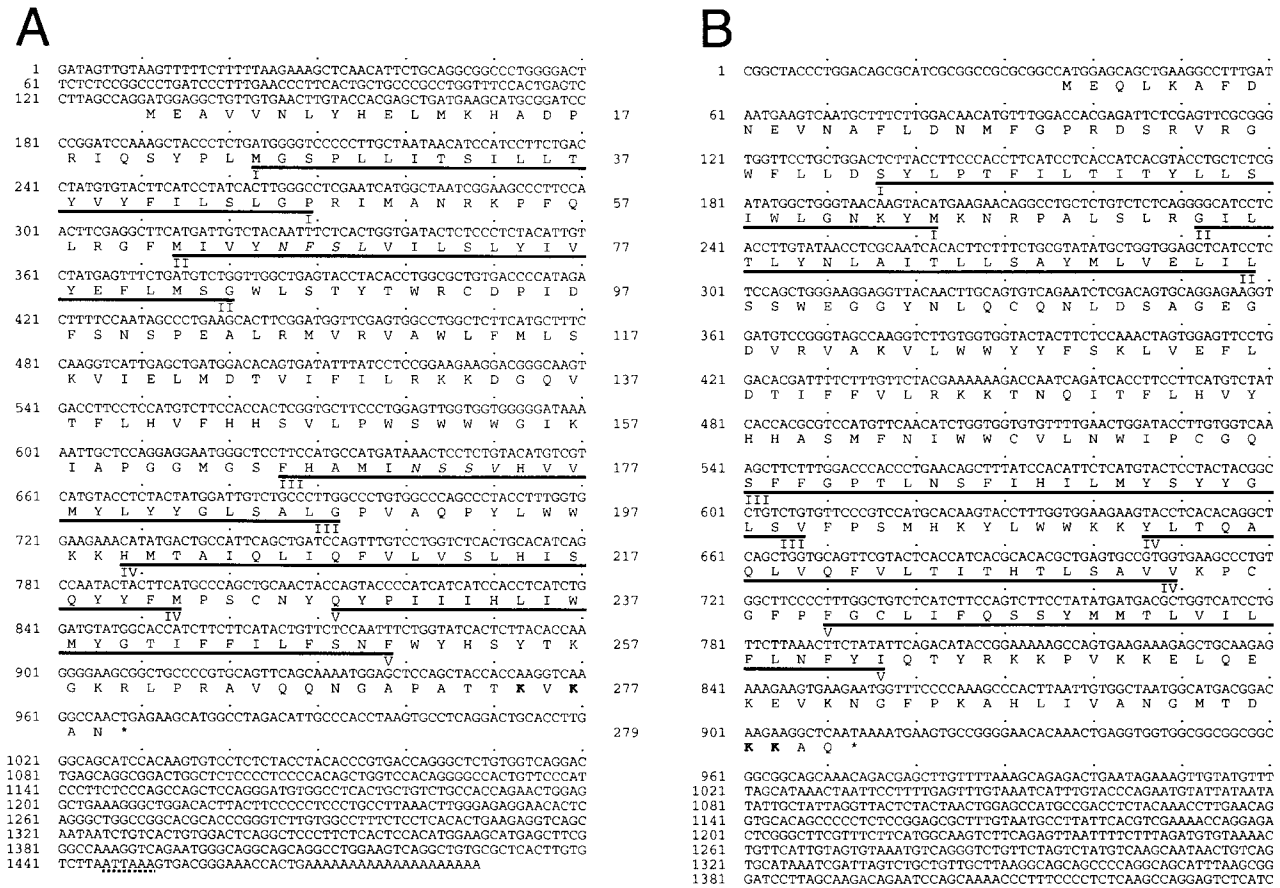

Figure 1. Nucleotide sequences of *Ssc1* (A) and *Ssc2* (B) cDNAs. Deduced amino acid sequences of the corresponding SSC polypeptides are shown below each open reading frame and putative membrane-spanning domains in both proteins are underlined and numbered with Roman numerals. Di-lysine motifs matching the ER retrieval signal are marked by bold letters. Polyadenylation signal consensus sequences are underlined with dashed lines. Sequence data have been deposited with the GenBank/EMBL/DDBJ data library under accession nos. AF170907 and AF170908.

sortium. After Northern hybridization of the clones to total RNA from several mouse tissues, we determined that both genes were expressed in the liver (data not shown). The full-length cDNAs were therefore obtained by PCR amplification from the liver RACE Ready cDNA library (Clontech). The nucleotide sequences of *Ssc1* and *Ssc2* cDNA are shown in Fig. 1. Although the length of the transcripts is markedly different (1.5 kb vs. 3.7 kb), the encoded polypeptides are very similar both in size and sequence. Amino acid sequence alignment of SSC1, SSC2, and CIG30 with homologous yeast polypeptides indicates that sequence identity in each mouse–mouse or mouse–yeast protein pair is ~30%, and they all contain 100% conserved motifs characteristic of this protein family, such as KXXEXXDT, FXHXXHH, HXXMYXYY, or TXXQXXQ (Fig. 2). The HXXHH consensus sequence is commonly found in fatty acid desaturases (Shanklin et al., 1994).

The SSC proteins are also similar to CIG30 in being

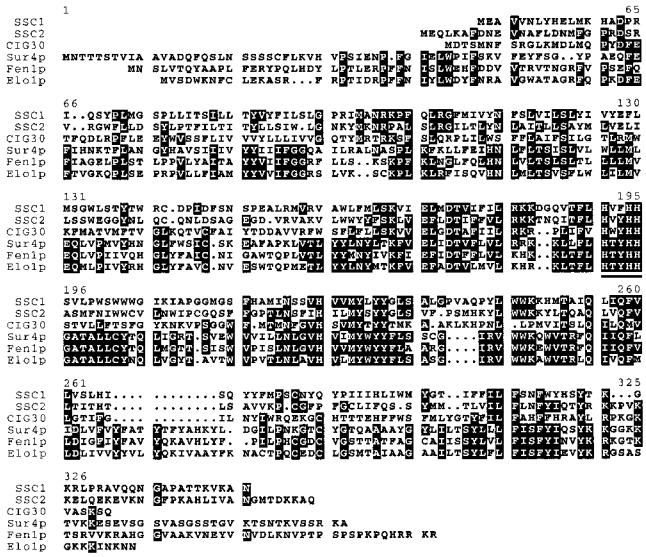

Figure 2. Amino acid sequence alignment of mouse and yeast Elo1p homologues. Amino acid positions conserved in at least 50% of the homologues are highlighted. The HXXHH motif, characteristic of desaturase/hydroxylase enzymes containing a diiron-oxo cluster (Fe-O-Fe), is underlined. The alignment was generated by the PileUp program.

highly hydrophobic. Hydropathy analyses by the GES algorithm (Engelman et al., 1986) suggest that they contain two NH_2-terminal transmembrane regions, followed by an amphiphilic region, and three to four COOH-terminal membrane-spanning regions (Fig. 3). Due to the long hydrophobic stretch in place of the third putative transmembrane region, it is less clear than in other homologues whether the total number of membrane-spanning regions is five or six (see also Oh et al., 1997; Tvrdik et al., 1997).

COOH-terminal sequences of both proteins contain an ER retention signal. The SSC1 polypeptide contains two lysine residues in positions −3 and −5 (KXKXX), and the COOH terminus of SSC2 matches the KKXX consensus sequence (−3 and −4; Fig. 1, A and B). Both signals have been shown to confer maximum ER retention/retrieval efficiency (Jackson et al., 1990). The ER retention signal in the CIG30 protein is rather weak, but it does have a lysine residue in the most critical −3 position (Fig. 2). We have not detected any other intracellular localization signals.

Previously, we have demonstrated that CIG30 is a glycoprotein (Tvrdik et al., 1997). However, in the SSC1 protein, both of the two potential *N*-glycosylation motifs (amino acid positions 66–69 and 171–174; Fig. 1 A) are buried in the putative membrane-spanning regions, and we found no *N*-glycosylation consensus sequence in SSC2, suggesting that the SSC proteins are not glycosylated. The absence of functional glycosylation sites in these proteins is also supported by our experiments in which we have seen no mobility shift of in vitro translated SSC polypeptides in the presence of canine microsomal membranes (not shown).

Expression of Ssc1, Ssc2, and Cig30 in Mouse Tissues

Northern blot analysis revealed that *Ssc1* was expressed in a broad variety of mouse tissues, whereas *Ssc2* expression, similar to *Cig30*, was rather tissue-specific (Fig. 4). The highest steady-state levels of *Ssc1* mRNA were found in stomach, lung, kidney, skin, and intestine, whereas white fat, liver, spleen, brain, brown fat, heart, and muscle showed moderate *Ssc1* expression. Only a very weak *Ssc1* mRNA signal was found in the testis. In contrast, the *Ssc2* mRNA levels in the testis were the highest of all tissues tested, followed by liver. Trace amounts of *Ssc2* transcript

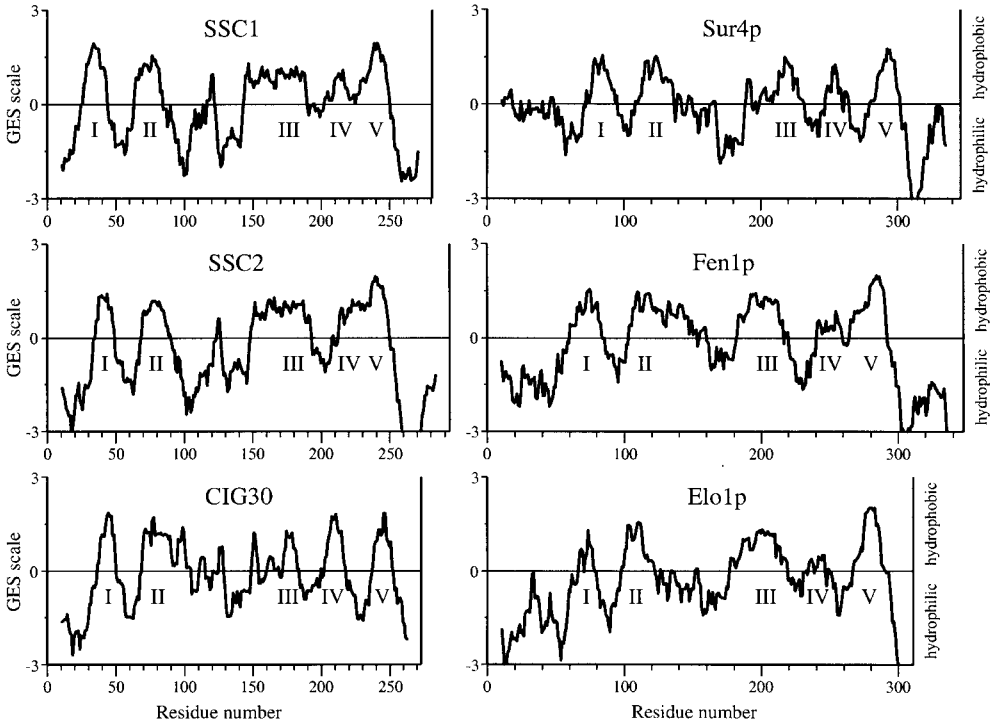

Figure 3. Hydropathy plots of SSC1, SSC2, CIG30, Sur4p, Fen1p, and Elo1p proteins. The plots were created by the PepPlot program using the Goldman, Engelman, and Steitz (GES) algorithm. The curves are averages of residue-specific hydrophobicity scales (the GES scales) over a window of 22 residues, positive values indicating hydrophobic regions. The putative transmembrane regions are numbered with Roman numerals. Abscissas in all graphs are drawn to the same scale.

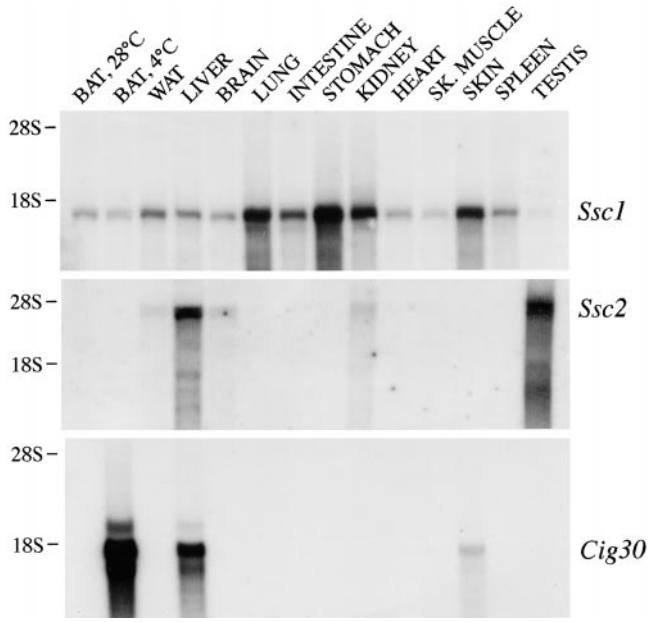

Figure 4. *Ssc1*, *Ssc2*, and *Cig30* mRNA levels in mouse tissues. Northern blot analyses were performed with 10 μg of total RNA isolated from the tissues indicated. BAT, 4°C, refers to RNA isolated from the brown adipose tissue of a mouse exposed to 4°C for 3 d. All other RNA samples were isolated from animals kept at thermoneutral temperature (28°C). WAT, White adipose tissue; SK. MUSCLE, skeletal muscle. The membranes were probed with ^{32}P-labeled cDNA fragments corresponding to open reading frames of *Ssc1*, *Ssc2*, and *Cig30*, respectively, and subsequently exposed to DuPont Cronex X-ray films for up to 1 wk. The positions of the ribosomal 28S and 18S RNAs are indicated on the left.

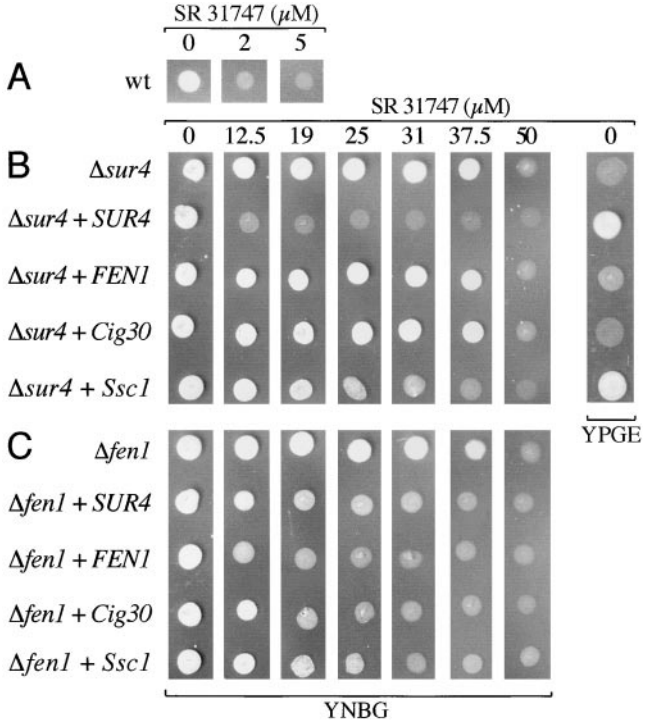

Figure 5. Rescue of SR 31747 sensitivity in the Δ*sur4* and Δ*fen1* yeast mutants by murine genes. A, Wild-type cells (EMA3). B, Δ*sur4* mutants transformed with expression plasmids containing the indicated genes. C, Δ*fen1* mutants transformed with the same range of expression vectors. Δ*sur4* and Δ*fen1* alone were transformed with the empty expression vector. The cells were incubated for 48 h on solid medium with increasing concentrations of SR 31747 (which are given in micromoles per liter above each series of transformants or wild-type cells). The media used were minimal synthetic medium supplemented with required amino acids (YNBG), or complex medium containing bactopeptone, yeast extract, glycerol, and ethanol (YPGE), as indicated below each section. Figure represents typical result of three independent experiments.

were also found in white fat, brain, and kidney. In agreement with our previous results, *Cig30* expression was detected in the liver and skin of thermoneutral mice, and it was strongly elevated in the brown fat of cold-exposed mice. It is noteworthy that neither *Ssc1* nor *Ssc2* expression was notably changed in that condition. The size of *Ssc1* and *Ssc2* mRNAs estimated from Northern blots was in good agreement with the size of their respective cDNAs.

Complementation of Yeast Mutants with Homologous Mouse Genes

Significant sequence similarities between *Cig30*, *Ssc1*, and *Ssc2* on the one hand, and *ELO1*, *FEN1*, and *SUR4* on the other, suggest a functional equivalency between the mouse and yeast gene families. To address this issue, we decided to investigate whether any of the mouse genes could complement for the yeast genes in Δ*sur4* or Δ*fen1* yeast mutants. It has been demonstrated that yeast vegetative growth could be inhibited by the sterol synthesis inhibitor SR 31747 in a dose-dependent manner (Silve et al., 1996). As shown in Fig. 5 A, growth of the parental yeast strain EMA3 was severely inhibited already by 2 μM SR 31747. After disruption of either *SUR4* or *FEN1*, however, SR 31747 tolerance was greatly enhanced and the resulting mutants were able to grow in the presence of >35 μM SR 31747. In the first series of experiments (Fig. 5 B), we transformed the Δ*sur4* mutant (EMY58) with yeast expression plasmids containing the genes of interest, and scored selected colonies for their ability to grow in increasing concentrations of SR 31747. Control transformation with *SUR4* restored SR 31747 sensitivity to the wild-type levels, whereas *FEN1* overexpression had no effect. In this expression system, *Ssc1* clearly conferred SR 31747 sensitivity, although less well than *SUR4*, and inhibited growth of the Δ*sur4* mutant at SR 31747 concentrations of 20–25 μM. Transformation with *Cig30* did not affect SR 31747 tolerance in this mutant. The second series of experiments (Fig. 5 C) performed in the Δ*fen1* mutant (EMA41) revealed that, predictably, *FEN1* restored wild-type SR 31747 sensitivity, but also that *SUR4* overexpression conferred nearly as low level of SR 31747 sensitivity as *FEN1*. Of the homologous mouse genes, *Cig30* consistently complemented the Δ*fen1* mutant best, conferring growth arrest at 15–20 μM SR 31747, but *Ssc1* could also mediate SR 31747 sensitivity at higher concentrations (25–30 μM). *Ssc2* complementation data were inconclusive in both yeast mutants (not shown).

In addition to being resistant to SR 31747, the Δ*sur4* mutant had also been shown to be unable to grow on glycerol/ethanol (Silve et al., 1996). In good agreement with the above results, *SUR4* or *Ssc1* rescued the Δ*sur4* mutant's ability to grow on glycerol/ethanol, whereas the other genes did not (Fig. 5 B, YPGE). Thus, our data support the view that *Ssc1* is functionally equivalent to *SUR4*, whereas *Cig30* appears to be similar to *FEN1*.

Since *Ssc2* failed to conclusively complement selected phenotypic defects in the Δ*sur4* and Δ*fen1* mutants, there remained a possibility that *Ssc2* could be functionally equivalent to *Elo1*. In contrast to *sur4* and *fen1*, the *elo1* mutant does not have any recognizable phenotype (Revardel et al., 1995). However, deletion of the fatty acid synthase gene uncovers its role in 14- to 16-carbon fatty acid chain elongation (Toke and Martin, 1996). To generate a suitable expression host, we disrupted the *FAS2* gene (encoding the α subunit of the fatty acid synthase) in the *elo1* mutant, and the resulting Δ*fas2*Δ*elo1* strain (EMA103) was transformed with the same range of expression vectors as before. All transformants were screened for their ability to grow on synthetic complete medium containing C_{14}. None of the transformed genes fully rescued the Δ*fas2*Δ*elo1* mutant, except for *ELO1* itself. A very weak growth was observed for the transformants expressing *SUR4*, *FEN1*, and *Cig30*. Neither *Ssc1* nor *Ssc2* allowed any growth at all (not shown). Thus, our data do not favor the possibility that *Ssc2* is a functional counterpart to *ELO1*.

Ssc1 Rescues Lethality of the sur4Δfen1 Double Mutant

Simultaneous loss of function in *SUR4* and *FEN1* leads to synthetic lethality (Revardel et al., 1995). Therefore, we asked if any of the mouse genes could support growth in the double mutant. We first transformed a *sur4* mutant (EMY22) to uracil prototrophy using an *Ssc1*-expressing vector. Transformed cells were mated with a *fen1* disruptant (EMA41). Diploids were induced to sporulate and single spore-derived colonies were isolated. Out of 67 Ura^+ colonies analyzed, one was correctly devoid of the wild-type versions of *SUR4* and *FEN1*, as confirmed by PCR analysis and DNA sequencing (not shown). This strain resisted the toxic effect of 25 μM SR 31747. To confirm that the growth rescue was dependent on *Ssc1*, we plated the cells onto medium containing 5′-fluoroorotic acid and uracil, a combination that only allows growth of Ura^- cells. As anticipated, the double mutant did not yield any plasmid-cured colonies. In a parallel control experiment, a single *sur4* mutant harboring the same *Ssc1*-expressing vector yielded plasmid-cured Ura^- segregants at a normal level (not shown). These results strongly suggested that *Ssc1* was capable of restoring viability in the *sur4*Δ*fen1* double mutant. After *Ssc1* loss, synthetic lethality of the double mutant could not be relieved by any of the media supplements we have tested, including VLCFA of 20, 22, and 24 carbon atoms, or ceramide.

We found no conclusive evidence for *Cig30* or *Ssc2* being able to restore proliferation in the double mutant. This could indicate that the mouse genes differ in their capacity to complement a more extensive biochemical defect in yeast. Accordingly, SSC1 appears to have the widest specificity and/or the highest activity.

Ssc1 Is Involved in Biosynthesis of C_{26} Fatty Acids and Sphingolipids

Recently, strong evidence has been provided that *ELO2/FEN1* and *ELO3/SUR4* are necessary for the synthesis of fatty acids of up to 24 and 26 carbons, respectively. As a result, Δ*sur4* and Δ*fen1* mutants have modified sphingolipid composition (Oh et al., 1997). These findings prompted us to investigate whether normal sphingolipid synthesis could be restored in these mutants by complementation with the mouse genes. The same range of yeast transformants used in the previous experiments were metabolically labeled with [^{3}H]serine, [^{3}H]sphinganine, or [^{3}H]inositol, and sphingolipids were isolated and separated by thin-layer chromatography. We found no marked difference in sphingolipid synthesis between wild-type and the Δ*fen1* strain (not shown). The Δ*sur4* mutant showed, however, a modified sphingolipid pattern as compared with the parental wild-type strain (Fig. 6). Most notably, the band corresponding to $M(IP)_2C$ was absent in the mutant. This band could not be restored by overexpression of the *FEN1* gene, but complementation with the wild-type *SUR4* gene restored the normal sphingolipid composition. Importantly, transformation with *Ssc1* restored the $M(IP)_2C$, but the rate of synthesis was below the rate seen in the wild-type (Fig. 6). *Ssc1* also restored normal sphingolipid synthesis in the *sur4*Δ*fen1* double mutant. However, neither *Ssc2* nor *Cig30* had any effect. As $M(IP)_2C$ contains almost exclusively cerotoyl (26:0) moieties, we concluded from this experiment that *Ssc1* has the capacity to catalyze the synthesis of cerotic acid and suggests it to be functionally equivalent to SUR4.

Ssc1 Is Markedly Downregulated in the Brains of the Myelin-deficient Mouse Mutants Quaking and Jimpy

Brains of the quaking and jimpy mouse mutants are marked by low VLCFA levels due to a reduced fatty acid elongation activity (Suneja et al., 1991). Therefore, we asked whether this decrease would be paralleled by a correspondingly low expression of the candidate gene for fatty acid elongase in the brain: the *Ssc1* gene. As seen in Fig. 7, the *Ssc1* mRNA levels in the brains of 18-d-old quaking mutants were reduced by 44% as compared with their normal littermates, while the actin mRNA levels in the same mutants were only insignificantly reduced by 12%. In the jimpy mutant, the cerebral *Ssc1* mRNA levels were downregulated even more dramatically, being reduced by 69%. Actin mRNA levels in the jimpy brain were only 16% below controls. Thus, reduced fatty acid chain elongation activities in the brains of quaking and jimpy mutants indeed appear to correlate with expression of the *Ssc1* gene.

Cig30 mRNA Induction Coincides with Enhanced Fatty Acid Chain Elongation Activity during Brown Fat Recruitment

In this mouse gene family, the most dramatic regulatory change so far observed is that of *Cig30* gene expression

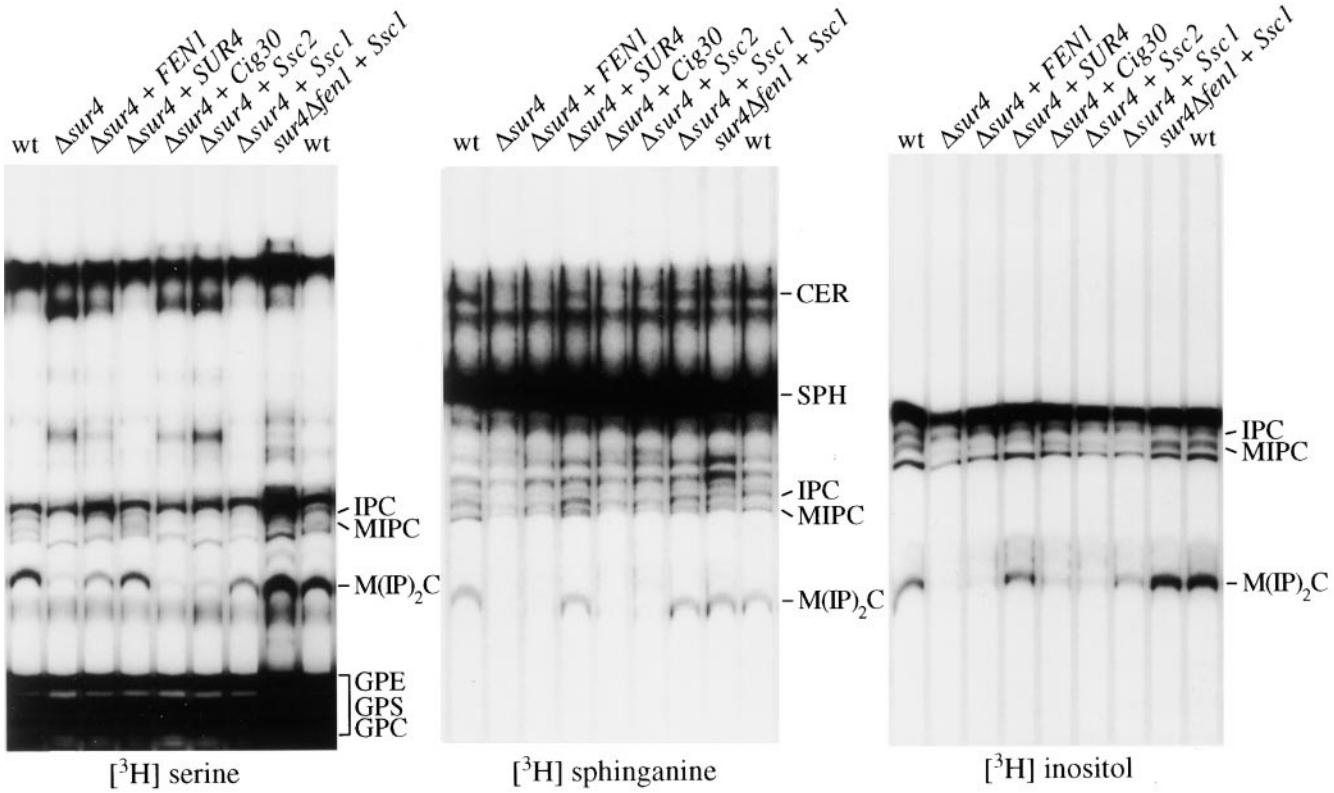

Figure 6. Mouse *Ssc1* restores glycosphingolipid levels in the Δ*sur4* yeast mutant. The Δ*sur4* yeast mutant cells were transformed either with the empty expression vector (Δ*sur4* alone), or with plasmids expressing *FEN1*, *SUR4*, *Cig30*, *Ssc2*, or *Ssc1*. Along with these transformants, the wild-type cells (EMA3) and the *sur4*Δ*fen1* double mutant transformed with *Ssc1* were metabolically labeled with [^{3}H]serine for 6 h, [^{3}H]sphinganine, or [^{3}H]inositol for 1.5 h. Total lipid extracts were prepared and separated by thin-layer chromatography. Before chromatography, [^{3}H]serine-labeled lipids shown here were subjected to mild alkaline hydrolysis with methylamine. The plates were treated with EN^{3}HANCE (New England Nuclear Life Science Products) and exposed to X-ray films for several weeks. The bands were identified by their relative mobility compared with radioactive standards ([^{3}H]sphinganine) and glycerolipid compounds were determined in parallel experiments on the basis of their sensitivity to methylamine (not shown). CER, Ceramide; GPC, glycerophosphorylcholine; GPE, glycerophosphorylethanolamine; GPS, glycerophosphorylserine; IPC, inositolphosphorylceramide; MIPC, mannose inositolphosphorylceramide; M(IP)$_2$C, mannose diinositolphosphorylceramide; SPH, sphinganine. Similar results were obtained in a duplicate experiment.

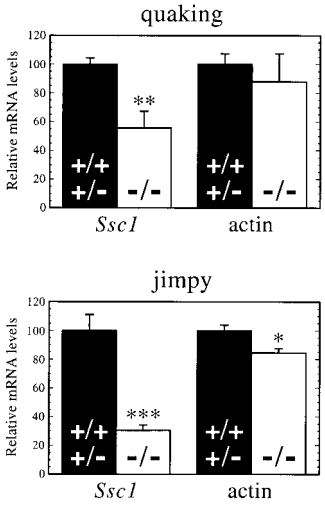

Figure 7. Ssc1 mRNA levels are severely decreased in the brains of mouse myelination mutants quaking and jimpy. Total RNA was isolated from the whole brains of 18-d-old phenotypic mutants (−/−) or their normal littermates (+/+ or +/−). 10 μg of RNA from each animal was analyzed by Northern blotting. After hybridization to *Ssc1* or actin cDNA probes, the membranes were quantified with a PhosphorImager (Molecular Dynamics). Each bar represents mean ± SEM of four animals. The means of the control groups were set to 100. Statistical differences between mutants and normal littermates were assessed by unpaired *t* test. *P* values: Quaking *Ssc1*, $P = 0.0120$ (**); quaking actin, $P = 0.5837$ (NS); jimpy *Ssc1*, $P = 0.0010$ (***); jimpy actin, $P = 0.0199$ (*).

during brown fat recruitment. Assuming that *Cig30* codes for a component of the fatty acid chain elongation system, we hypothesized that the induction of *Cig30* expression would be paralleled by an increase in the fatty acid chain elongation activity. To test this, we isolated microsomal membranes from brown fat of thermoneutral and cold-stimulated mice, and determined fatty acid chain elongation capacity in these samples. Table II shows that elongation activity was indeed significantly increased in the brown fat of mice stimulated by low ambient temperature (4°C) for 3 d, relative to thermoneutral controls. The highest increase (4.7×) was observed when palmitoyl CoA (16:0) was used as substrate. Lower values were obtained with arachidoyl CoA (20:0) as substrate (4.3×). The elongation activity on lignoceroyl CoA (24:0) was induced least and the increase was insignificant. Hence, our data demonstrate that elongation of at least two acyl CoA substrates is strongly enhanced in brown fat during recruitment, consistent with the idea that this increase could be due, in part, to the observed induction of *Cig30* expression (Tvrdik et al., 1997).

Table II. Brown Fat Microsomal Fatty Acyl Chain Elongation Activity in Warm- and Cold-acclimated Mice

Substrate	BAT (28°C)	BAT (4°C)	Relative increase in cold	*P* value
	pmol Mal-CoA/min/mg prot		×	
palmitoyl CoA (C_{16})*	1.80 ± 0.64	8.50 ± 1.51	4.7	0.004
arachidoyl CoA (C_{20})*	0.37 ± 0.05	1.57 ± 0.52	4.3	0.065
lignoceroyl CoA (C_{24})‡	0.33 ± 0.06	1.12 ± 0.56	3.4	0.229

Total fatty acid chain elongation activities in the presence of NADPH were determined in microsomal fractions prepared from brown adipose tissue (BAT) of mice either kept at thermoneutral temperature (28°C) or exposed to the cold for 3 d (4°C). Specific activity was expressed as picomoles of radioactive malonyl CoA (Mal-CoA) incorporated into hydrophobic long chain fatty acid fraction by 1 mg of microsomal protein in 1 min. Statistical significance of the increase was determined by unpaired *t* test.
*Value represents the mean ± SEM of two experiments performed in triplicate.
‡Value represents the mean ± SEM of one experiment performed in triplicate.

Discussion

An initial clue about the function of the *Cig30* and *Ssc* genes was obtained by sequence comparisons, which revealed homology with the yeast *ELO* gene family. There are only three members of this family in the yeast genome. It is not known how many paralogs are present in mammalian genomes, but the fact that *C. elegans* contains at least six similar genes (Tvrdik et al., 1997) suggests that the number of mouse paralogs presented here is not final. We were unable to identify any clear yeast–mouse orthologous pair by phylogenic analysis. If anything, *Cig30* appears to be more closely related to the yeast genes, whereas both *Ssc* genes seem evolutionarily more distant (Tvrdik, P., unpublished data). Neither could we recognize any common protein domains other than the HXXHH motif previously noticed (Toke and Martin, 1996; Oh et al., 1997). This histidine-rich motif is found in diiron-oxo proteins, such as ribonucleotide reductase or various fatty acid desaturases. Histidine residues act together with aspartate and glutamate to coordinate the Fe-O-Fe cluster, which is believed to receive electrons from either cytochrome b_5 or a cytochrome b_5-like domain in an NAD(P)H-dependent way (Fox et al., 1994; Shanklin et al., 1994). This similarity implicates *ELO1* homologues in a redox type of reaction. Therefore, it is reasonable to assume that this group of enzymes could catalyze one or both of the reduction reactions in fatty acid elongation, i.e., conversion of β-ketoacyl CoA to β-hydroxyacyl CoA or reduction of trans-2-enoyl CoA to the saturated acyl CoA derivative. Further support for this view comes from plant research. Although VLCFA in plants, in contrast to the animal kingdom, are almost solely used as constituents of surface coverings, such as wax, the chemistry of fatty acid elongation is fundamentally similar. Several putative condensing enzymes (which catalyze the first rate-limiting step in fatty acid elongation leading to β-ketoacyl CoA formation) have been cloned in plants (Millar and Kunst, 1997; Millar et al., 1999; Todd et al., 1999) and shown to stimulate VLCFA synthesis after expression in various heterologous systems, including yeast (Millar and Kunst, 1997). None of the plant condensing enzymes, however, share significant homology with SSC1, SSC2, CIG30, Sur4p, Fen1p, or Elo1p. Thus, if we exclude the possibility that two unrelated fatty acid chain elongation systems have evolved in plants and animals, sequence comparisons suggest that CIG30 and the SSC proteins are not involved in β-ketoacyl CoA synthesis, but possibly in β-ketoacyl CoA or trans-2-enoyl CoA reduction.

A major fraction of noncytoplasmic fatty acid chain elongation activity resides in the membranes of the ER. Consistent with their role in VLCFA synthesis, both Sur4p and Fen1p were localized by immunofluorescence of HA epitope-tagged proteins to intracellular structures, which were identified as ER or early Golgi apparatus (David et al., 1998). Further, as shown in Fig. 1, the COOH-terminal sequences of the SSC1 and SSC2 polypeptides contain perfect consensi for ER retrieval signals, suggesting that the mouse proteins reside in the ER as well. In contrast, we initially localized the CIG30 protein by GFP tagging primarily to the plasma membrane (Tvrdik et al., 1997). However, since the GFP protein was linked to the COOH terminus of CIG30, this discrepancy could possibly be explained by inefficient retrieval of the CIG30–GFP fusion protein from the Golgi due to a misplacement of the ER localization motif. As a result, most of the fusion protein could perhaps have been mistargeted to the plasma membrane, presumably in synergy with the weak ER retrieval signal in CIG30 (lysine residues in the –3 and –7 positions, compare Fig. 2).

Moreover, we have earlier established that the single *N*-glycosylation consensus site in the NH_2 terminus of CIG30 is glycosylated (Tvrdik et al., 1997), indicating that the NH_2-terminal domain sees the inner side of ER. Given that all Elo1p homologues are integral membrane proteins sharing a similar topology with five plausible transmembrane regions (Oh et al., 1997; Tvrdik et al., 1997; Fig. 3), it can be predicted that their NH_2 termini are located in the ER lumen, whereas their COOH-terminal segments are exposed to the cytoplasm.

Complementation in yeast mutants allowed us to uncover specific functional relationships between the yeast and mouse genes, which could not be detected by sequence comparisons. Thus, our experiments clearly demonstrate that *Ssc1* is functionally orthologous to *SUR4*, because in all complementation tests, it restored a wild-type–like phenotype to the Δ*sur4* mutant. Specifically, we showed that *Ssc1* expression is able to recover the synthesis of $M(IP)_2C$ (see Fig. 6). Oh et al. (1997) attributed low glycosphingolipid levels in the *elo3/sur4* mutant to impaired VLCFA metabolism. Indeed, even though the total levels of long chain fatty acid were ~20% increased in the *elo3/sur4* mutant, C_{26} species were entirely absent. Under normal circumstances, αOH-C_{26} is the predominant fatty acid found in $M(IP)_2C$ (Dickson, 1998). This suggests that SSC1, unlike the other mouse paralogs, is able to utilize C_{24} CoA as a substrate for elongation. Given the virtu-

ally ubiquitous expression of the *Ssc1* gene in the mouse (Fig. 4), it can be inferred that most mammalian tissues are endowed with an enzymatic capacity to synthesize VLCFA up to C_{26} or more. Interestingly, the *Ssc1* mRNA levels were particularly high in the stomach, lung, kidney, skin, and intestine. Common to all these tissues is that they separate compartments widely differing in water content. Therefore, it is conceivable that higher SSC1 levels are necessary to bring about sufficient VLCFA production in order to reduce the water permeability of the barrier epithelia (Zeidel, 1996).

Further linking *Ssc1* to mammalian VLCFA metabolism, we show in Fig. 7 that quaking and jimpy mouse mutants have dramatically decreased cerebral *Ssc1* mRNA levels. Both mutants are easily recognizable as they develop intense tremor at the age of about two weeks as a result of severe demyelination of the central nervous system. Although the molecular mechanisms causing demyelination in each mutant are very different, in both cases they eventually lead to massive oligodendrocyte death (Hardy, 1998; Vela et al., 1998). Among the multiple lipid defects known to take place during brain development in the mutants, fatty acid elongation activity has been investigated by several groups in great detail. In their study, Suneja et al. (1991) showed that microsomal fatty acid chain elongation activity in the brains of quaking mutant mice relative to controls were 45 and 52% decreased when using arachidoyl CoA (C_{20}) and behenoyl CoA (C_{22}) as substrates, respectively. Similar values in jimpy were 77 and 81% below controls. This correlates strikingly well with 44% decrease in quaking *Ssc1* mRNA levels and 69% decrease in jimpy *Ssc1* mRNA levels that we report in this study, suggesting that the severity of the elongation defect is proportional to the reduction in *Ssc1* expression. However, Suneja et al. (1991) also found that in both mutants only the condensation activity was reduced, whereas reduction and dehydration steps were unaffected, implicating a defect in the condensing enzyme. This would disagree with a role for *Ssc1* in a reduction reaction, which we tentatively propose on the basis of sequence comparisons.

Cig30 appears functionally equivalent to *FEN1* as it confers a similar level of sensitivity to the inhibitor of ergosterol biosynthesis (as depicted in Fig. 5 C). Interpretation of this experiment is more complex, because overexpression of *SUR4* could also increase SR 31747 sensitivity in the *fen1* mutant. It has been previously observed that both enzymes have overlapping activities in such a way that *SUR4* can partially substitute for *FEN1*, but not vice versa (Silve et al., 1996). In the light of the tentative biochemical function of these proteins, this observation could probably be explained by a broader substrate specificity of the Sur4p enzyme. Interestingly, *Ssc1* was also able to partially restore SR 31747 sensitivity in the *fen1* mutant (Fig. 5 C), corroborating the hypothesis that *Ssc1*/*SUR4* and *Cig30*/*FEN1* are orthologous pairs. Further, there is a structural similarity between *Cig30* and *FEN1* in having a single *N*-glycosylation site in their proximal NH_2 termini (El-Sherbeini and Clemas, 1995; Tvrdik et al., 1997). In terms of sphingolipid synthesis, however, we could not consistently detect any effect of *FEN1* disruption, which would have allowed an assessment of substitution with Cig30. This could be considered in line with the theoretical prediction, because the complex yeast glycosphingolipids contain mainly C_{26}, which cannot be made by Fen1p (Oh et al., 1997). Nevertheless, both Oh et al. (1997) and David et al. (1998) observed a significant (>60%) reduction in MIPC and $M(IP)_2C$ levels as a result of *FEN1* deletion. This inconsistency could be partly attributable to the genetic variability of different yeast strains that may differ in the relative amount of fatty acids that *FEN1* contributes to the total VLCFA pool.

In mice, *Cig30* expression is tightly associated with activity of brown adipose tissue (Tvrdik et al., 1997). Within several days upon appropriate stimulation, such as low ambient temperature, brown fat *Cig30* mRNA becomes very abundant (Fig. 4). Here, we show that brown fat recruitment is also accompanied by concomitantly elevated microsomal fatty acid chain elongation activity (Table II). Although the magnitude is different (an approximate fivefold increase in elongation activity as opposed to a >200-fold increase in *Cig30* transcripts), our results are not inconsistent with a role for *Cig30* in brown fat microsomal fatty acid elongation. Our finding also raises questions as to what is the physiological purpose of enhanced fatty acid elongation in brown fat recruitment. A possibility is that the elevated fatty acid elongation activity furnishes fatty acids for the needs of greater membrane production. Brown fat recruitment is known to bring about tissue hyperplasia, which employs mechanisms such as accelerated cell proliferation and mitochondriogenesis (Trayhurn and Nicholls, 1986). Obviously, these processes require augmented phospholipid synthesis. It is also possible that the elevated *Cig30* expression is specifically involved in sphingolipid synthesis, as it has been shown that the amount of the major ganglioside in brown fat, GM_3, is significantly increased during the process of brown fat recruitment (Kuroshima and Ohno, 1990).

Presently, we are unable to assign any specific activity to *Ssc2*. It conferred no significant complementation in the yeast mutants, including the Δ*fas2elo1* disruptant. Thus, it remains an open question whether mammals possess the elusive *ELO1*-like enzymatic activity, which in wild-type cells completely overlaps with fatty acid synthase. However, the failure of *Ssc2* to complement could have been due to other factors, such as a lack of proper interaction with other proteins in the yeast elongation complex, or an insufficient level of expression. It is also possible that SSC2 could have a different substrate specificity. *Ssc2* expression is particularly high in the testis (Fig. 4), one of the richest sources of polyenoic long chain fatty acids in the body, which might suggest that SSC2 specifically interacts with polyunsaturated fatty acid species.

In summary, extreme hydrophobicity of the enzymes involved in microsomal fatty acid elongation has hindered isolation and characterization of these complexes. We have circumvented this obstacle by using the approach of reverse genetics and have cloned novel mammalian genes that are strongly implicated in VLCFA synthesis. Our results reveal similarities between yeast and mammalian fatty acid elongation and support the view that several mammalian membrane-bound elongation complexes exist with different sets of subunits. Some subunits are expressed in a tissue-specific manner, allowing VLCFA synthesis to be finely tuned in different tissues and different

stages of development. By cloning the first components, our work takes the initial step towards the possibility of reconstituting membrane-bound fatty acid chain elongation complexes in vitro.

We thank Birgitta Leksell for technical assistance, Patrick Jara for the pNK451 vector, and Evelyne Liauzun for the *neo* gene.

This work was supported by grants from the Jeansson Foundation and from the Swedish Natural Science Research Council, and from the Swedish Medical Research Council.

Submitted: 4 February 2000
Revised: 13 March 2000
Accepted: 15 March 2000

References

Alani, E., L. Cao, and N. Kleckner. 1987. A method for gene disruption that allows repeated use of URA3 selection in the construction of multiply disrupted yeast strains. *Genetics*. 116:541–545.

Bernert, J.J., and H. Sprecher. 1979. Solubilization and partial purification of an enzyme involved in rat liver microsomal fatty acid chain elongation: beta-hydroxyacyl-CoA dehydrase. *J. Biol. Chem*. 254:11584–11590.

Bourre, J.M., J.M. Paturneau, O.L. Daudu, and N.A. Baumann. 1977. Lignoceric acid biosynthesis in the developing brain. Activities of mitochondrial acetyl-CoA-dependent synthesis and microsomal malonyl-CoA chain-elongating system in relation to myelination. Comparison between normal mouse and dysmyelinating mutants (quaking and jimpy). *Eur. J. Biochem*. 72:41–47.

Cinti, D.L., L. Cook, M.N. Nagi, and S.K. Suneja. 1992. The fatty acid chain elongation system of mammalian endoplasmic reticulum. *Prog. Lipid. Res*. 31:1–51.

Clarke, N.G., and R.M. Dawson. 1981. Alkaline O leads to N-transacylation. A new method for the quantitative deacylation of phospholipids. *Biochem. J*. 195:301–306.

David, D., S. Sundarababu, and J.E. Gerst. 1998. Involvement of long chain fatty acid elongation in the trafficking of secretory vesicles in yeast. *J. Cell Biol*. 143:1167–1182.

Desfarges, L., P. Durrens, H. Juguelin, C. Cassagne, M. Bonneu, and M. Aigle. 1993. Yeast mutants affected in viability upon starvation have a modified phospholipid composition. *Yeast*. 9:267–277.

Devereux, J., P. Haeberli, and O. Smithies. 1984. A comprehensive set of sequence analysis programs for the VAX. *Nucleic Acids Res*. 12:387–395.

Dickson, R.C. 1998. Sphingolipid functions in *Saccharomyces cerevisiae*: comparison to mammals. *Annu. Rev. Biochem*. 67:27–48.

Durrens, P., E. Revardel, M. Bonneu, and M. Aigle. 1995. Evidence for a branched pathway in the polarized cell division of *Saccharomyces cerevisiae*. *Curr. Genet*. 27:213–216.

El-Sherbeini, M., and J.A. Clemas. 1995. Cloning and characterization of GNS1: a *Saccharomyces cerevisiae* gene involved in synthesis of 1,3-beta-glucan in vitro. *J. Bacteriol*. 177:3227–3234.

Engelman, D.M., T.A. Steitz, and A. Goldman. 1986. Identifying nonpolar transbilayer helices in amino acid sequences of membrane proteins. *Annu. Rev. Biophys. Chem*. 15:321–353.

Fox, B.G., J. Shanklin, J. Ai, T.M. Loehr, and L.J. Sanders. 1994. Resonance raman evidence for an Fe-O-Fe center in stearoyl-ACP desaturase. Primary sequence identity with other diiron-oxo proteins. *Biochemistry*. 33:12776–12786.

García-Arranz, M., A.M. Maldonado, M.J. Mazón, and F. Portillo. 1994. Transcriptional control of yeast plasma membrane H(+)-ATPase by glucose. Cloning and characterization of a new gene involved in this regulation. *J. Biol. Chem*. 269:18076–18082.

Gietz, D., A. St. Jean, R.A. Woods, and R.H. Schiestl. 1992. Improved method for high efficiency transformation of intact yeast cells. *Nucleic Acids Res*. 20: 1425.

Hakomori, S., and Y. Igarashi. 1995. Functional role of glycosphingolipids in cell recognition and signaling. *J. Biochem. (Tokyo)*. 118:1091–1103.

Hanada, K., M. Nishijima, M. Kiso, A. Hasegawa, S. Fujita, T. Ogawa, and Y. Akamatsu. 1992. Sphingolipids are essential for the growth of Chinese hamster ovary cells. Restoration of the growth of a mutant defective in sphingoid base biosynthesis by exogenous sphingolipids. *J. Biol. Chem*. 267:23527–23533.

Hannun, Y.A. 1996. Functions of ceramide in coordinating cellular responses to stress. *Science*. 274:1855–1859.

Hanson, B.A., and R.L. Lester. 1980. The extraction of inositol-containing phospholipids and phosphatidylcholine from *Saccharomyces cerevisiae* and *Neurospora crassa*. *J. Lipid Res*. 21:309–315.

Hardy, R.J. 1998. Molecular defects in the dysmyelinating mutant quaking. *J. Neurosci. Res*. 51:417–422.

Jackson, M.R., T. Nilsson, and P.A. Peterson. 1990. Identification of a consensus motif for retention of transmembrane proteins in the endoplasmic reticulum. *EMBO (Eur. Mol. Biol. Organ.) J*. 9:3153–3162.

Kuroshima, A., and T. Ohno. 1990. Cold–induced and postnatal changes in brown adipose tissue ganglioside levels. *Jpn. J. Physiol*. 40:57–64.

Ladeveze, V., C. Marcireau, D. Delourme, and F. Karst. 1993. General resistance to sterol biosynthesis inhibitors in *Saccharomyces cerevisiae*. *Lipids*. 28:907–912.

Lester, R.L., G.B. Wells, G. Oxford, and R.C. Dickson. 1993. Mutant strains of *Saccharomyces cerevisiae* lacking sphingolipids synthesize novel inositol glycerophospholipids that mimic sphingolipid structures. *J. Biol. Chem*. 268: 845–856.

Millar, A.A., and L. Kunst. 1997. Very-long-chain fatty acid biosynthesis is controlled through the expression and specificity of the condensing enzyme. *Plant J*. 12:121–131.

Millar, A.A., S. Clemens, S. Zachgo, E.M. Giblin, D.C. Taylor, and L. Kunst. 1999. CUT1, an arabidopsis gene required for cuticular wax biosynthesis and pollen fertility, encodes a very-long-chain fatty acid condensing enzyme. *Plant Cell*. 11:825–838.

Oh, C.S., D.A. Toke, S. Mandala, and C.E. Martin. 1997. ELO2 and ELO3, homologues of the *Saccharomyces cerevisiae* ELO1 gene, function in fatty acid elongation and are required for sphingolipid formation. *J. Biol. Chem*. 272: 17376–17384.

Poulos, A. 1995. Very long chain fatty acids in higher animals: a review. *Lipids*. 30:1–14.

Revardel, E., M. Bonneau, P. Durrens, and M. Aigle. 1995. Characterization of a new gene family developing pleiotropic phenotypes upon mutation in *Saccharomyces cerevisiae*. *Biochim. Biophys. Acta*. 1263:261–265.

Shanklin, J., E. Whittle, and B.G. Fox. 1994. Eight histidine residues are catalytically essential in a membrane-associated iron enzyme, stearoyl-CoA desaturase, and are conserved in alkane hydroxylase and xylene monooxygenase. *Biochemistry*. 33:12787–12794.

Silve, S., P. Leplatois, A. Josse, P.H. Dupuy, C. Lanau, M. Kaghad, C. Dhers, C. Picard, A. Rahier, M. Taton, et al. 1996. The immunosuppressant SR 31747 blocks cell proliferation by inhibiting a steroid isomerase in *Saccharomyces cerevisiae*. *Mol. Cell. Biol*. 16:2719–2727.

Simons, K., and E. Ikonen. 1997. Functional rafts in cell membranes. *Nature*. 387:569–572.

Spiegel, S., and A.J. Merrill. 1996. Sphingolipid metabolism and cell growth regulation. *FASEB J*. 10:1388–1397.

Suneja, S.K., M.N. Nagi, L. Cook, and D.L. Cinti. 1991. Decreased long-chain fatty acyl CoA elongation activity in quaking and jimpy mouse brain: deficiency in one enzyme or multiple enzyme activities? *J. Neurochem*. 57:140–146.

Testi, R. 1996. Sphingomyelin breakdown and cell fate. *Trends Biochem. Sci*. 21:468–471.

Todd, J., B.D. Post, and J.G. Jaworski. 1999. KCS1 encodes a fatty acid elongase 3-ketoacyl-CoA synthase affecting wax biosynthesis in *Arabidopsis thaliana*. *Plant J*. 17:119–130.

Toke, D.A., and C.E. Martin. 1996. Isolation and characterization of a gene affecting fatty acid elongation in *Saccharomyces cerevisiae*. *J. Biol. Chem*. 271: 18413–18422.

Trayhurn, P., and D.G. Nicholls. 1986. Brown Adipose Tissue. Edward Arnold Ltd., London. 374 pp.

Tvrdik, P., A. Asadi, L.P. Kozak, J. Nedergaard, B. Cannon, and A. Jacobsson. 1997. Cig30, a mouse member of a novel membrane protein gene family, is involved in the recruitment of brown adipose tissue. *J. Biol. Chem*. 272: 31738–31746.

Vela, J.M., B. Gonzalez, and B. Castellano. 1998. Understanding glial abnormalities associated with myelin deficiency in the jimpy mutant mouse. *Brain Res. Rev*. 26:29–42.

Wells, G.B., and R.L. Lester. 1983. The isolation and characterization of a mutant strain of *Saccharomyces cerevisiae* that requires a long chain base for growth and for synthesis of phosphosphingolipids. *J. Biol. Chem*. 258:10200–10203.

Wertz, P.W. 1992. Epidermal lipids. *Semin. Dermatol*. 11:106–113.

Zeidel, M.L. 1996. Low permeabilities of apical membranes of barrier epithelia: what makes watertight membranes watertight? *Am. J. Physiol*. F243–F245.